

8th Japan-China-Korea Workshop on Microgravity Sciences  
for Asian Microgravity Pre-Symposium

## Synthesis of Giant Magnetostrictive Iron-rich Sm-Fe Alloy by Unidirectional Solidification in Microgravity

Takeshi OKUTANI<sup>1</sup>, Hiromichi ONO<sup>1</sup> and Hideaki NAGAI<sup>2</sup>

### Abstract

Sm-Fe magnetostrictive material was produced by unidirectional solidification of Sm-Fe alloy with atomic ratio from 1/2 to 2/17 in microgravity within  $\pm 4 \times 10^{-3}g$  for 1.43s obtained using 10-m drop tower and with fluctuating gravity between 0.1 and 0.02g obtained by parabolic flight.  $SmFe_2$  and a small amount of  $Sm_2Fe_{17}$  as well as Fe were formed from unidirectional solidification in microgravity of Sm-7Fe alloy, obtained using the drop tower and parabolic flight. The structure consisted of sheet dendrites of  $SmFe_2$  and Fe-rich Sm-Fe layers between the sheet dendrites having no gaps with an orientation along the solidification direction. A crystalline orientation of  $\langle 111 \rangle$  of  $SmFe_2$  along the solidification direction was found in the products formed in microgravity using the drop tower, but not in those using parabolic flight. The formation mechanisms of  $SmFe_2$  sheet dendrites can be explained by microsegregation caused by the lack of convection in melt in microgravity. In contrast,  $Sm_2Fe_{17}$  and a small amount of Fe were formed in normal-gravity, and the resulting structure consisted of sheet dendrites without orientation. Magnetostriction of -3328ppm at the outer magnetic fields of 0.12T was achieved on a sample synthesized by unidirectional solidification of Sm-7Fe in microgravity obtained using the drop tower.

### 1. Introduction

Laves phase compounds such as  $TbFe_2$ ,  $SmFe_2$  and  $Tb_{0.3}Dy_{0.7}Fe_{1.9}$  (Terfenol-D) are known as giant magnetostrictive materials which have a magnetostriction more than 1000ppm by applying several hundreds mT of working magnetic fields. High-performance giant magnetostrictive materials with high magnetostriction and low working magnetic fields have a columnar or sheet structure and  $\langle 111 \rangle$  crystallographic orientation along the magnetostriction direction or single crystal. We successfully produced in  $TbFe_2$ <sup>1), 2), 3)</sup>,  $SmFe_2$ <sup>4)</sup> and Terfenol-D<sup>5), 6)</sup> with sheet dendrite structure and  $\langle 111 \rangle$  orientation along the solidification direction by unidirectional solidification in magnetic field (no magnetic field for  $SmFe_2$ ) in short-duration microgravity ( $\mu g$ ) of  $10^{-4}g$  for 10s obtained using a 490-m drop shaft and  $10^{-3}g$  for 1.43s obtained using a 10-m drop tower. From the results of unidirectional solidification for magnetostrictive materials such as  $TbFe_2$ ,  $SmFe_2$  and Terfenol-D in  $\mu g$  of  $10^{-3}g$  for 1.43s obtained using the 10-m drop tower, the nucleation developed in the initial stage of solidification affected sheet dendrites aligned with the solidification direction and  $\langle 111 \rangle$  orientation.

For  $Tb_xDy_{1-x}Fe_y$  ( $0.28 < x < 0.32$ ,  $1.95 < y < 1.99$ ) which is the same Laves phase magnetostrictive intermetallic compound as  $SmFe_2$ , rare-earth elements such as Tb and Dy are contained at more than the stoichiometric ratio,  $(Tb+Dy)/Fe=1/2$  atomic ratio, in the intermetallic compound. Verhoeven et al. reported that the form of a rare-earth microconstituent varied within a sample at

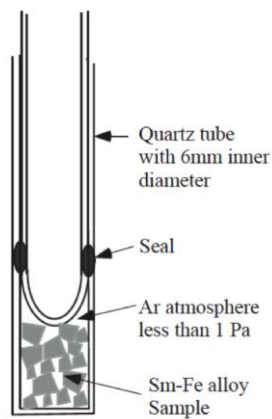
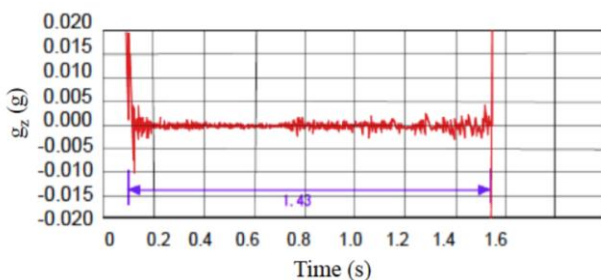
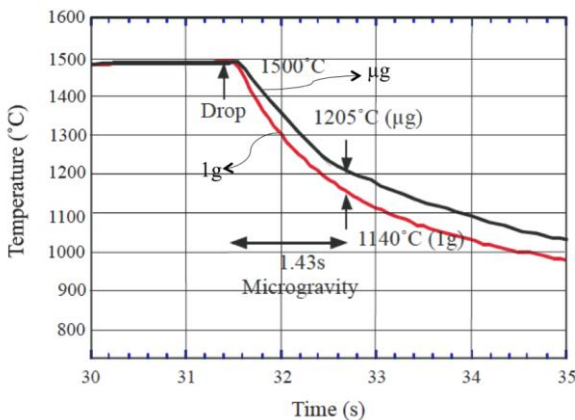
some locations; it was a eutectic mixture of  $RFe_2$  ( $R=Tb, Dy$ ) plus R metal, formed by a divorced eutectic reaction.<sup>7)</sup> They reported that the rare-earth phase is interconnected throughout the crystalline volume,<sup>8)</sup> and it is apparently the presence of this ductile metal phase containing rich Tb and Dy that reduces the brittleness, although pure  $Tb_{0.3}Dy_{0.7}Fe_2$  compound is extremely brittle. However, inner stresses derived from magnetostriction caused cracks in the matrix of giant magnetostrictive materials. After measuring the magnetostriction, we observed cracks perpendicular to the solidified direction.<sup>5)</sup> Fe metal is thought to be more ductile than R metals. If giant magnetostrictive materials consisting of sheet dendrites of magnetostrictive-material phase with Fe-rich phase between the dendrites can be produced, the resulting materials will be tough against inner stress. However, iron-rich  $Tb_{0.3}Dy_{0.7}Fe_Z$  and  $SmFe_Z$  ( $Z > 2.01$ ) have not yet been reported.

In this report, unidirectional solidification of Sm-Fe alloys with Sm/Fe atomic ratios ranging from 1/2 to 2/17 in  $\mu g$  was investigated to produce high-performance Sm-Fe giant magnetostrictive materials consisting of  $SmFe_2$  sheet dendrites with Fe-rich phase between the sheets.  $\mu g$  experiments were carried out using a 10-m drop tower, providing  $\mu g$  of  $\pm 4 \times 10^{-3}g$  for 1.43s, and parabolic flight, providing fluctuating gravity between 0.1 and -0.02g for 20s, to investigate the effect of gravity on the metallurgical structure of these products.

### 2. Experimental

1 Graduate School of Environment and Information Sciences, Yokohama National University, 79-7 Tokiwadai, Hodogaya-ku, Yokohama 240-8501, Japan

2 National Institute of Advanced Industrial Science and Technology, 1-1-1 Higashi, Tsukuba 305-8565, Japan  
(E-mail: okutani@ynu.ac.jp)


**Fig. 1** Sample reactor

**Fig. 2** Level in the vertical direction ( $g_z$ ) obtained by the 10m drop tower.

**Fig. 3** Cooling profile of the contact surface of Sm-Fe samples in drop tower experiment and normal gravity.

## 2.1 Samples

Santoku Metal Co. provided Sm-7Fe alloy prepared by melting in an induction furnace at a temperature of 1400°C in an argon atmosphere at a pressure of 0.1MPa. Sm-2Fe, Sm-3Fe and 2Sm-17Fe alloys were prepared by adding Sm (Turning, 99.9% purity, Wako Pure Chemical Industries, Ltd.) or Fe (99.9% purity, Kojundo Chemical Laboratory Co., Ltd.) to Sm-7Fe alloy. Each piece of Sm-7Fe alloy, Sm or Fe with a diameter less than 1mm was weighed and mixed to create Sm/Fe atomic ratios of 1/2, 1/3 and 2/17. A 1gr Sm-Fe sample was placed in the sample holder (**Fig. 1**).

## 2.2 Drop Tower Experiments

In the drop tower experiments, an infrared heater was used to heat the sample from room temperature to 1500°C within 30 seconds. The solidification equipment was dropped upon reaching 1500°C, at which point the sample melted completely; heating was stopped 0.2s after the start of the drop. At the same time, the reactor was shifted from the center of the IR furnace to the outside of the furnace to initiate contact between the flat bottom of the reactor and a 50×50×0.5mm copper plate that was set outside the furnace. Unidirectional solidification was initiated from the melt plate on the flat bottom of the reactor through contact with the copper plate. **Figure 2** illustrated the  $\pm 4 \times 10^{-3} g$  level in the vertical direction ( $g_z$ ) obtained using the 10m-drop tower, as measured by an accelerometer (CXLO2LF3, Crossbow Technology, Inc.). **Figure 3** plots the cooling curves for unidirectional solidification in  $\mu g$  and in normal gravity (1g). Cooling from 1500 to 1205°C ( $\Delta 295^\circ C$ ) in  $\mu g$  and cooling from 1500 to 1140°C ( $\Delta 360^\circ C$ ) in 1g were attained within 1.43s. No supercooling or recalescence was observed during solidification of the Sm-Fe melts.

## 2.3 Parabolic Flight Experiments

In the parabolic flight experiments, the unidirectional solidification apparatus, the samples, and the experimental procedure were the same as that used with the drop tower. The parabolic flights were carried out by G-II (Diamond Air Service, Inc.). **Figure 4** indicates the  $\mu g$  level in the vertical direction ( $g_z$ ) and the cooling curve for unidirectional solidification in  $\mu g$  obtained during the parabolic flight. The  $\mu g$  level obtained in the parabolic flight fluctuated from 0.1g to -0.02g. Cooling from

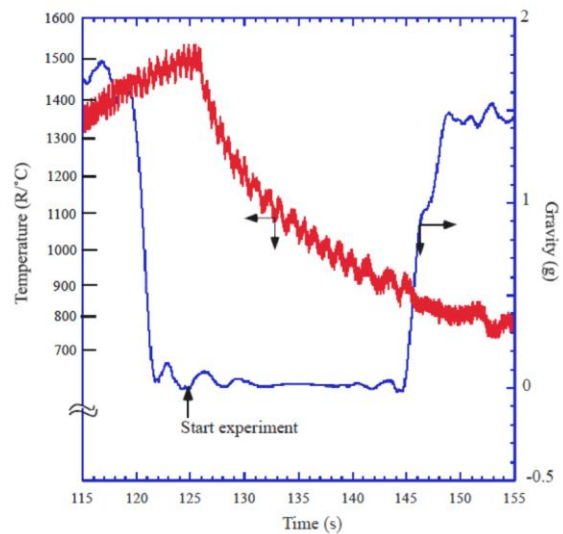

**Fig. 4** Typical cooling curve and microgravity level of Sm-Fe sample in parabolic flight.

Table 1. Crystalline compounds of samples solidified from the Sm-Fe melts with atomic ratios of 1/2, 1/3, 1/7, and 2/17 in ground, drop tower and parabolic flight experiments detected by XRD.

Composition of alloy	Sm-2Fe	Sm-3Fe	Sm-7Fe	2Sm-17Fe
Ground exp. (1g)	SmFe <sub>2</sub> <sup>+</sup>	SmFe <sub>3</sub> <sup>+</sup> SmFe <sub>2</sub>	Sm <sub>2</sub> Fe <sub>17</sub> <sup>+</sup> Fe	Sm <sub>2</sub> Fe <sub>17</sub> <sup>+</sup> Fe
Drop tower exp. ( $\pm 4 \times 10^{-3}$ g, 1.43s)	SmFe <sub>2</sub> <sup>+</sup>	SmFe <sub>3</sub> <sup>+</sup> , SmFe <sub>2</sub> Sm <sub>2</sub> Fe <sub>17</sub>	SmFe <sub>2</sub> <sup>+</sup> , Sm <sub>2</sub> Fe <sub>17</sub> , Fe Low crystalline orientation*	Sm <sub>2</sub> Fe <sub>17</sub> <sup>+</sup> Fe
Parabolic flight exp. (0.1~ -0.02g, 20s)	SmFe <sub>2</sub> <sup>+</sup>	SmFe <sub>3</sub> <sup>+</sup> , SmFe <sub>2</sub> , Sm <sub>2</sub> Fe <sub>17</sub>	SmFe <sub>2</sub> <sup>+</sup> , Sm <sub>2</sub> Fe <sub>17</sub> , Fe	Sm <sub>2</sub> Fe <sub>17</sub> <sup>+</sup> Fe
Predicted crystalline phases from phase diagram	SmFe <sub>2</sub>	SmFe <sub>3</sub>	SmFe <sub>3</sub> + Sm <sub>2</sub> Fe <sub>17</sub>	Sm <sub>2</sub> Fe <sub>17</sub>

<sup>+</sup>) Crystalline compound having primary XRD peaks.

<sup>\*</sup>) Only <111> of SmFe<sub>2</sub> was aligned along the solidification direction.

1500 to 860°C ( $\Delta 640^\circ\text{C}$ ) in  $\mu\text{g}$  was attained within 20s. No supercooling or recalescence was observed during the solidification of the Sm-Fe melts.

## 2.4 Evaluation

The solidified sample was then embedded in epoxy resin and cut in half. Both pieces were carefully embedded in order to align the cross-section perpendicular and parallel to the line of the cooling (solidification) direction for analysis. The polished samples were observed via optical microscopy (Olympus; BX51M) to investigate their microstructures. The sample was analyzed by X-ray diffraction (Rigaku LINT), using a sample rotation system of 30rpm to determine the crystal structure and crystalline orientation. The Sm and Fe distributions of the starting alloys and solidified products were observed by SEM-XMA (JOEL; JED-2140 V2). Magnetostriction measurements were carried out by determining the elongation of the sample along with the cooling (solidification) direction with an applied to the magnetic field ranging from 0 to 0.12 T using a highly precise measuring sensor with 0.1 $\mu\text{m}$  resolutions.

## 3. Results and Discussion

### 3.1 Crystalline Phases of Solidified Products

Table 1 lists the crystalline phases produced by unidirectional solidification of Sm-2Fe, Sm-3Fe, Sm-7Fe and 2Sm-17Fe melt in 1g and  $\mu\text{g}$  obtained using the drop tower and the parabolic flights.

The solidified product of the Sm-2Fe melt was SmFe<sub>2</sub> only. According to the phase diagram of the Sm-Fe binary system in Fig. 5 and the cooling curves shown in Figs. 3 and 4, the Sm-2Fe sample is solidified to Sm<sub>2</sub>Fe<sub>17</sub>+Liquid during  $\mu\text{g}$  obtained

using the drop tower and to SmFe<sub>2</sub> via SmFe<sub>3</sub>+Liquid during the following 1g. The Sm-2Fe solidified in parabolic flight is formed of SmFe<sub>2</sub> via Sm<sub>2</sub>Fe<sub>17</sub>+Liquid and SmFe<sub>3</sub>+Liquid during  $\mu\text{g}$ . The result, in which SmFe<sub>2</sub> was the only solidified product of the Sm-2Fe in  $\mu\text{g}$  and 1g, demonstrates that SmFe<sub>2</sub> forms rapidly and that the no convection of melt in  $\mu\text{g}$  does not affect the SmFe<sub>2</sub> formation.

SmFe<sub>3</sub> is the final product of solidification for the Sm-3Fe according to the phase diagram shown in Fig. 5, but SmFe<sub>3</sub> and SmFe<sub>2</sub> were formed from solidification in 1g and Sm<sub>2</sub>Fe<sub>17</sub> was formed from solidification in  $\mu\text{g}$  in addition to SmFe<sub>3</sub> and SmFe<sub>2</sub>. This result indicates that the reaction rate of SmFe<sub>3</sub> from Sm<sub>2</sub>Fe<sub>17</sub>+Liquid is fast and that SmFe<sub>2</sub> was formed by micro heterogeneity in the melt because of its higher stability compared with SmFe<sub>3</sub>, although SmFe<sub>2</sub> is not formed from the melt of Sm-3Fe from the phase diagram in Fig. 5. Sm<sub>2</sub>Fe<sub>17</sub> was found in  $\mu\text{g}$  in addition to SmFe<sub>3</sub> and SmFe<sub>2</sub>. The melt (Liquid in the phase diagram) surrounding Sm<sub>2</sub>Fe<sub>17</sub> developed a lack of Sm during the reaction of Fe+Liquid into Sm<sub>2</sub>Fe<sub>17</sub>+Liquid because there was no convection of melt in  $\mu\text{g}$ , and the reaction was thus terminated to form Sm<sub>2</sub>Fe<sub>17</sub>.

The products resulting from the solidification of the Sm-7Fe were Sm<sub>2</sub>Fe<sub>17</sub> and Fe in 1g and SmFe<sub>2</sub>, Sm<sub>2</sub>Fe<sub>17</sub>, and Fe in  $\mu\text{g}$ . These products differ from the prediction of the phase diagram, in which the Sm-7Fe melt is solidified to Sm<sub>2</sub>Fe<sub>17</sub>+Liquid via Fe+Liquid during free-fall using the drop tower, and to Sm<sub>2</sub>Fe<sub>17</sub>+SmFe<sub>3</sub> via Sm<sub>2</sub>Fe<sub>17</sub>+Liquid in the following 1g, and in which Sm<sub>2</sub>Fe<sub>17</sub>+SmFe<sub>3</sub> is formed via Fe+Liquid and Sm<sub>2</sub>Fe<sub>17</sub>+Liquid in  $\mu\text{g}$  in parabolic flight. There appears to be no SmFe<sub>3</sub> in the products solidified in 1g and  $\mu\text{g}$ , since the Sm-7Fe is similar to 2Sm-17Fe. In  $\mu\text{g}$ , that is, without convection in melts, Fe nuclei are formed in the melts during the

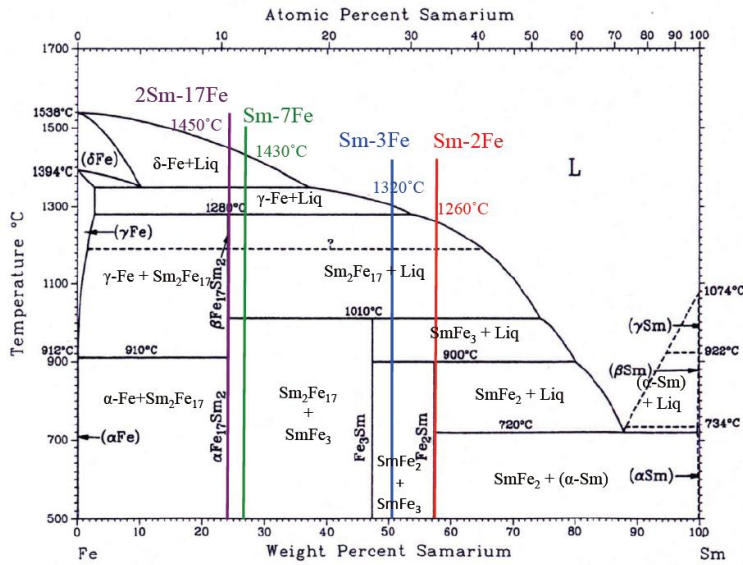


Fig. 5. Phase diagram of Sm-Fe binary system.  
 M.P. of  $\text{Sm}_2\text{Fe}_{17}$ : 1280°C, M.P. of  $\text{SmFe}_3$ : 1010°C,  
 M.P. of  $\text{SmFe}_2$ : 900°C

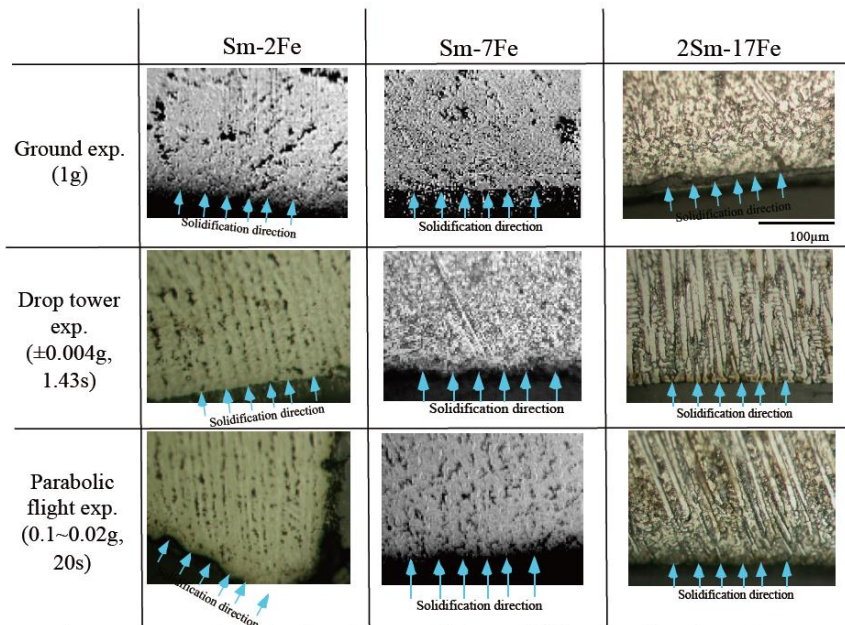


Fig. 6. Microstructure of polished surface parallel to solidification direction of Sm-Fe samples with 1/2, 1/7 and 2/17 atomic ratios.  
 The Sm-Fe samples with 1/7 and 2/17 atomic ratios were etched by nital solution (5vol % $\text{HNO}_3$ +95vol% $\text{C}_2\text{H}_5\text{OH}$ ).

initial stage of solidification. These Fe nuclei react with Sm in the melts to form  $\text{Sm}_2\text{Fe}_{17}$ . The Sm concentration of the melt near solid  $\text{Sm}_2\text{Fe}_{17}$  increases with the growth of  $\text{Sm}_2\text{Fe}_{17}$  nuclei because of Fe consumption by  $\text{Sm}_2\text{Fe}_{17}$  after which a stable  $\text{SmFe}_2$  phase appears in the Sm-rich melt. The height of the Fe XRD peaks increased with the solidification in 1g, in parabolic flight and in the drop tower, in descending order of the quality of  $\mu\text{g}$ , from 1g to  $\pm 4 \times 10^{-3}\text{g}$ . The  $\text{SmFe}_2$  XRD peaks of the solidified product in the drop tower were much higher than those obtained in parabolic flight. The formation of  $\text{SmFe}_2$  requires  $\mu\text{g}$

and the amount of  $\text{SmFe}_2$  is affected by the quality of  $\mu\text{g}$ . Fe formation stems from the lack of Sm due to the formation of  $\text{SmFe}_2$ . If  $\text{Sm}_2\text{Fe}_{17}$  and  $\text{SmFe}_2$  are formed from the Sm-7Fe,  $\text{SmFe}_2$  constitutes 37.5mol% of the products. If  $\text{SmFe}_2$ ,  $\text{Sm}_2\text{Fe}_{17}$  and Fe of the same content as  $\text{Sm}_2\text{Fe}_{17}$  are formed from Sm-7Fe,  $\text{SmFe}_2$  constitutes 44.4mol% of the products because the height of Fe XRD peaks obtained in the drop-tower experiments were the same as those of  $\text{Sm}_2\text{Fe}_{17}$  XRD peaks. The  $\langle 111 \rangle$  of  $\text{SmFe}_2$  in the solidified product obtained in the drop-tower experiments

Table 2. Microstructure and structural orientation along solidification direction of samples. Solidification from the Sm-Fe melts with atomic ratios of 1/2, 1/3, 1/7 and 2/17 in ground, drop tower and parabolic flight experiments.

Composition of alloy	Sm-2Fe	Sm-3Fe	Sm-7Fe	2Sm-17Fe
Ground exp. (1g)	Sheet dendrite No orientation	Sheet dendrite No orientation	Sheet dendrite No orientation	Dendrite No orientation
Drop tower exp. ( $\pm 4 \times 10^{-3}$ g, 1.43s)	Sheet dendrite Orientation	Sheet dendrite Orientation	Sheet dendrite Orientation (60°)	Dendrite Orientation
Parabolic flight exp. (0.1~ -0.02g, 20s)	Sheet dendrite Orientation (60°)	Sheet dendrite Partial orientation (60°)	Sheet dendrite Orientation	Dendrite Orientation (60°)

was aligned along the solidification direction. The orientation of the  $\text{SmFe}_2$  will be discussed later.

The 2Sm-17Fe sample is solidified to  $\text{Sm}_2\text{Fe}_{17}$  via Fe+Liquid in 1g and  $\mu\text{g}$  in both the drop tower and the parabolic flight. This result matches the prediction in the Sm-Fe phase diagram in **Fig. 5**.

### 3.2 Microstructure of Solidified Products

**Figure 6** depicts the microstructure of a polished surface parallel to the solidification direction in the Sm-2Fe, Sm-7Fe, and 2Sm-17Fe samples. The microstructure and the structural orientation along the solidification direction for samples solidified in Sm-2Fe, Sm-3Fe, Sm-7Fe, and 2Sm-17Fe melts in ground, drop-tower and parabolic-flight experiments are summarized in **Table 2**.

A sheet dendrite structure was observed in the Sm-2Fe, Sm-3Fe, and Sm-7Fe samples, and a dendrite columnar structure was observed in the 2Sm-17Fe sample. The sheet dendrite and dendrite structures were oriented along the solidification direction for the samples solidified in  $\mu\text{g}$  obtained using both the drop tower and the parabolic flights, but the sheet dendrite of the solidified Sm-7Fe sample obtained using the drop tower, the sheet dendrite of the solidified Sm-2Fe obtained during the parabolic flight, and the dendrite of the solidified 2Sm-17Fe obtained during the parabolic flight had a 60-degree slope to the surface contacting the copper plate. Gaps between the sheet dendrites were observed in the Sm-2Fe and Sm-3Fe solidified samples in 1g and  $\mu\text{g}$ . Voids were observed in the Sm-7Fe samples solidified in 1g and in  $\mu\text{g}$  during parabolic flight. No gaps or voids were observed in the Sm-7Fe sample solidified in  $\mu\text{g}$  obtained using the drop tower or in the 2Sm-17Fe sample solidified in 1g and  $\mu\text{g}$ .

The microstructure of the solidified Sm-7Fe sample in  $\mu\text{g}$  obtained using the drop tower consisted of sheet dendrite of  $\text{SmFe}_2$  with filler between the sheet dendrites and with  $\langle 111 \rangle$  of the  $\text{SmFe}_2$  aligned with the solidification direction. **Figs. 7** and **8** present SEM images and the Sm and Fe line profiles of Sm-7Fe

solidified in  $\mu\text{g}$  obtained using the drop tower and in 1g. A surface parallel to the solidification direction was observed. The dark part is Fe-rich phase, and the white part is  $\text{SmFe}_2$  sheet dendrites. The Fe-rich phase appears like dendrite, and is assumed to be  $\text{Sm}_2\text{Fe}_{17}$  dendrite. The direction of the sheet dendrite and dendrite is aligned at 60° to the surface contacting the Cu plate in the solidified sample in  $\mu\text{g}$  obtained using the drop tower. There are no gaps between the sheet dendrites, but there are a few small voids. In contrast, the direction of the Fe-rich phase dendrite is random and the  $\text{Sm}_2\text{Fe}_{17}$  in the white part is dendrite of small size and random direction in the sample solidified in 1g.

The solidification mechanism of Sm-7Fe melt is thought to be that Fe nuclei are formed in the melt in the first stage of solidification, the Fe nuclei react with Sm in the melt to form  $\text{Sm}_2\text{Fe}_{17}$  + melt, and the  $\text{Sm}_2\text{Fe}_{17}$  grows into columnar dendrite (as primary arms of dendrite). The growth of  $\text{Sm}_2\text{Fe}_{17}$  consumes the Fe component in the Sm-7Fe melt, and the melts between the  $\text{Sm}_2\text{Fe}_{17}$  columnar dendrites thus become Sm-rich because there is no convection in  $\mu\text{g}$ . Sm-rich melts solidify to sheet dendrite  $\text{SmFe}_2$ . Finally, microstructure of solidified Sm-7Fe melt in  $\mu\text{g}$  consists of sheet dendrites of  $\text{SmFe}_2$  with Fe-rich phase such as  $\text{Sm}_2\text{Fe}_{17}$  between the sheet dendrites as shown in **Fig. 9**. As a result, the microstructure is derived from microsegregation in  $\mu\text{g}$ .

In unidirectional solidification of Sm-7Fe in 1g,  $\text{SmFe}_2$  is not formed but  $\text{Sm}_2\text{Fe}_{17}$  and Fe are. Fe nuclei were formed in the initial stage of solidification, and then  $\text{Sm}_2\text{Fe}_{17}$ +Liquid is formed via Fe+Liquid, as seen in the phase diagram in **Fig. 5**. Microsegregation did not occur because of convection in the melt in 1g, so  $\text{SmFe}_2$  did not form from the Sm-7Fe alloy melt.

The sheet surface of the  $\text{SmFe}_2$  dendrites formed by solidification of Sm-7Fe melt in  $\mu\text{g}$  obtained during parabolic flight was rough compared with that in  $\mu\text{g}$  obtained using the drop tower (**Fig. 6**). The  $\mu\text{g}$  level fluctuated from 0.1 to -0.02g in parabolic flight but that of the drop tower was  $\pm 4 \times 10^{-3}$ g.

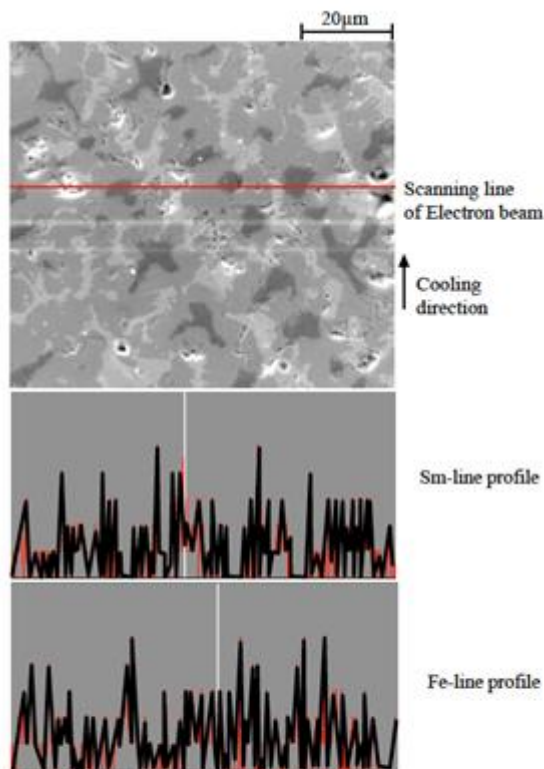


Fig. 7. SEM and Sm- and Fe-line profiles of Sm-7Fe solidified in  $\mu g$  obtained by the drop tower.

The surface parallel to the cooling (solidification) direction was observed.

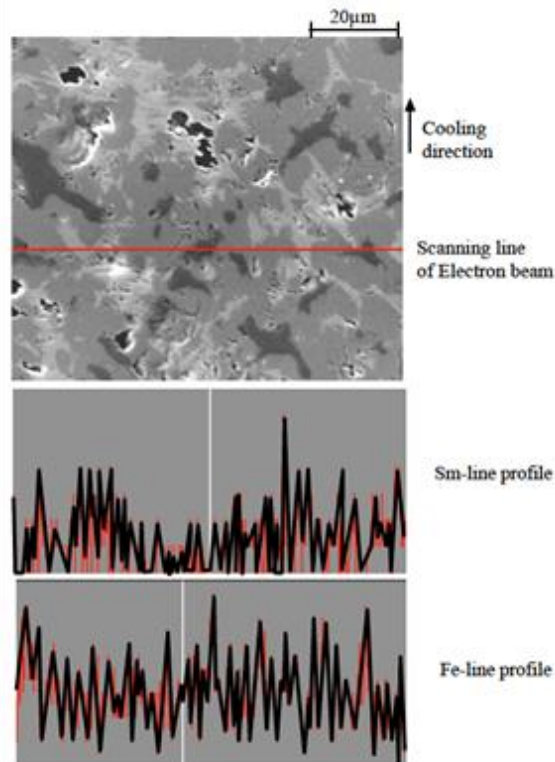


Fig. 8. SEM and Sm- and Fe-line profiles of Sm-7Fe solidified in normal gravity.

The surface parallel to the cooling (solidification) direction was observed.

The fluctuation of  $\mu g$  during unidirectional solidification affected the morphology and crystalline orientation of the solidified product.

### 3.3 Magnetostriction

Magnetostrictions at the outer magnetic field of 0.12T in the samples solidified unidirectionally Sm-2Fe, Sm-3Fe, Sm-7Fe, and 2Sm-17Fe melts in 1g, using the drop tower and during parabolic flight, as seen in **Table 3**. The samples of Sm-2Fe solidified in  $\mu g$  obtained using the drop tower and parabolic flight and the Sm-3Fe in  $\mu g$  obtained using the drop tower had gaps between the sheet dendrites, and therefore the magnetostriction was very low (-80 to -200ppm). The samples solidified from Sm-2Fe in 1g, from Sm-3Fe in 1g and  $\mu g$  obtained by parabolic flight, and from Sm-7Fe in 1g had voids and a range of magnetostriction from -600 to -1200ppm. The products from 2Sm-17Fe were mainly  $Sm_2Fe_{17}$  where the magnetostriction was low because  $Sm_2Fe_{17}$  is a permanent-magnet phase with high coercivity. The magnetostriction of the solidified product from Sm-7Fe in  $\mu g$  obtained using the drop tower was -3328ppm. The microstructure of the magnetostrictive materials consisted of  $SmFe_2$  sheet dendrites with Fe-rich phase between the sheet dendrites and without gaps or voids. The sheet dendrites were aligned along the solidification direction, and the

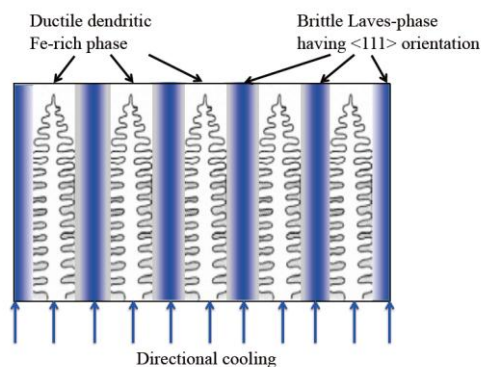


Fig. 9. Schematic of iron-rich Sm-7Fe by unidirectional solidification in  $\mu g$ .

crystalline orientation of  $SmFe_2$  with the solidification direction was <111>, which was the crystalline axis direction with the highest magnetostriction among the crystalline axes. The magnetostriction of the solidified product from Sm-7Fe in  $\mu g$  obtained during parabolic flight was -1776ppm. The surface of the  $SmFe_2$  sheet dendrite was rough and voids existed in the sample due to  $\mu g$  fluctuating from 0.1 to -0.02g.

To synthesize  $SmFe_2$  sheet dendrites with Fe-rich phase between sheet dendrites and without gaps or voids, alignment of the  $SmFe_2$  sheet dendrites with the magnetostriction direction

Table 3 Magnetostriction at outer magnetic field of 0.12T of samples solidified unidirectionally from Sm-2Fe, Sm-3Fe, Sm-7Fe, and 2Sm-17Fe melts in normal gravity, drop tower and parabolic flight.

	Sm-2Fe	Sm-3Fe	Sm-7Fe	2Sm-17Fe
Normal gravity (1g)	-1054	-1003	-583	-813
Drop tower ( $10^{-3}$ g, 1.43s)	-191	-200	-3328	-281
Parabolic flight (rd. $10^{-2}$ g, 20s)	-76.4	-1186	-1776	-1100

(ppm)

and a  $\langle 111 \rangle$  crystalline orientation of  $\text{SmFe}_2$  with the magnetostriction direction, a high-quality g-level are required.

#### 4. Conclusions

Sm-Fe magnetostrictive material was produced by the unidirectional solidification of Sm-2Fe, Sm-3Fe, Sm-7Fe and 2Sm-17Fe alloys in  $\mu\text{g}$  within  $\pm 4 \times 10^{-3}$ g for 1.43s obtained using a 10-m drop tower and with gravity fluctuating between 0.1 and -0.02g, obtained during parabolic flight. The structure of high-performance Sm-Fe giant magnetostrictive materials must consist of  $\text{SmFe}_2$  sheet dendrites with Fe-rich phase between the sheet dendrites, without gaps, and must have an orientation of the  $\text{SmFe}_2$  sheet dendrites toward the solidification direction and an alignment of the  $\langle 111 \rangle$  crystalline axes of  $\text{SmFe}_2$  with the solidification direction. By using unidirectional solidification of Sm-7Fe alloy melt in  $\mu\text{g}$  obtained using the 10-m drop tower, we successfully obtained such a structure. The product of unidirectional solidification of Sm-7Fe melt in  $\mu\text{g}$  consisted of sheet dendrites of  $\text{SmFe}_2$  with Fe-rich Sm-Fe layers between the sheet dendrites, without gaps and with an orientation of the  $\text{SmFe}_2$  sheet dendrites along the solidification direction. A crystalline orientation of  $\langle 111 \rangle$  of  $\text{SmFe}_2$  along the solidification direction was found in the products in  $\mu\text{g}$ , and the  $\text{SmFe}_2$  content in the product solidified in  $\mu\text{g}$  increased with increasing Fe content. The formation mechanisms of  $\text{SmFe}_2$  sheet dendrites can be explained by microsegregation caused by the lack of convection in melt in  $\mu\text{g}$ . The quality of  $\mu\text{g}$  plays a very important role in synthesizing a magnetostrictive material

having such a structure. Magnetostriction of -3328ppm was obtained at the outer magnetic field of 0.12T on the sample synthesized by unidirectional solidification in  $\pm 4 \times 10^{-3}$ g obtained using the drop tower.

#### Acknowledgement

This research was supported by Grand-based Research Program for Space Utilization promoted by the Japan Space Forum.

#### References

- 1) H. Minagawa, K. Kamada, T. Konishi, T. Tsurue, H. Nagai, Y. Nakata, M. Sasamori, and T. Okutani: *J. Magn. Magn. Mater.*, **234**(3) (2001) 437.
- 2) T. Okutani, Y. Nakata and H. Nagai: *Ann. N.Y. Acad. Sci.*, **1027** (2004) 158.
- 3) T. Okutani, Y. Nakata, H. Nagai and M. Mamiya: *Microgravity Science & Technology*, **XVI**/1 (2005) 84.
- 4) T. Okutani, H. Nagai, M. Mamiya, M. Shibuya, and M. Castillo: *Ann. N.Y. Acad. Sci.*, **1077** (2006) 146.
- 5) H. Minagawa, K. Kamada, H. Nagai, Y. Nakata and T. Okutani: *J. Magn. Magn. Mater.*, **248** (2002) 230.
- 6) T. Okutani, H. Nagai and M. Mamiya: *Ann. N.Y. Acad. Sci.*, **1161** (2009) 437.
- 7) J.D. Verhoeven, A.J. Bevolo, D.T. Peterson, H.H. Baker, O.D. McMasters and E.D. Gibson: *Metallography*, **18** (1985) 277.
- 8) O.D. McMasters, J.D. Verhoeven and E.D. Gibson: *J. Magn. Magn. Mater.*, **54-57** (1986) 849.

(Received 22 Sept. 2010; Accepted 22 Jun. 2011)